PB80-167216

REPORT NO.
UCB/EERC-79/31
DECEMBER 1979

EARTHQUAKE ENGINEERING RESEARCH CENTER

3D BEAM-COLUMN ELEMENT (TYPE 2-PARALLEL ELEMENT THEORY) FOR THE ANSR-II PROGRAM

by

ALI RIAHI
GRAHAM H. POWELL
DIGAMBAR P. MONDKAR

Report to Sponsor:
National Science Foundation
Grant ENV76-04262

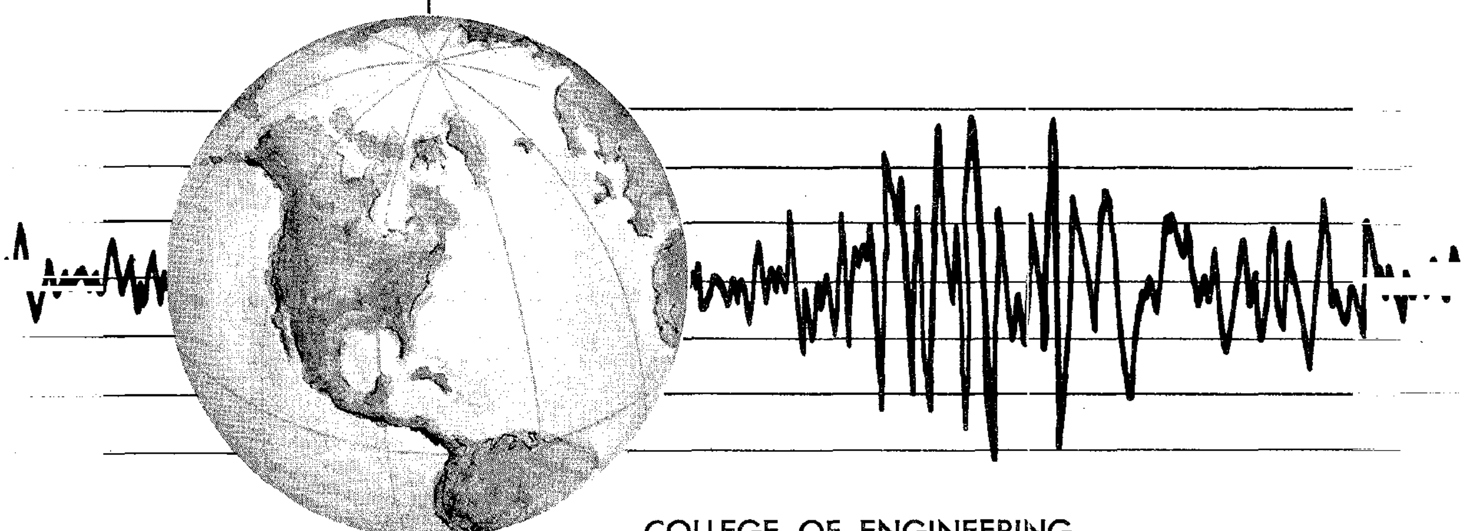

COLLEGE OF ENGINEERING

UNIVERSITY OF CALIFORNIA · Berkeley, California

BIBLIOGRAPHIC DATA SHEET	1. Report No. NSF/RA-790363	2.	3. Recipient's Accession No. PB 80 167216
4. Title and Subtitle 3D Beam-Column Element (Type 2-Parallel Element Theory) for the ANSR-II Program			5. Report Date December 1979 6.
7. Author(s) A. Riahi, G.H. Powell and D.P. Mondkar			8. Performing Organization Rept. No. UCB/EERC-79/31
9. Performing Organization Name and Address Earthquake Engineering Research Center University of California, Richmond Field Station 47th and Hoffman Blvd. Richmond, California 94804			10. Project/Task/Work Unit No. 11. Contract/Grant No. ENV76-04262
12. Sponsoring Organization Name and Address National Science Foundation 1800 G. Street, N.W. Washington, D.C. 20550			13. Type of Report & Period Covered 14.

15. Supplementary Notes

16. Abstracts

This report describes a three dimensional inelastic beam-column element developed for the ANSR-II program. The report contains a description of the element characteristics, the theoretical formulation, and a computer program user's guide.

17. Key Words and Document Analysis. 17a. Descriptors

17b. Identifiers/Open-Ended Terms

17c. COSATI Field/Group

18. Availability Statement	19. Security Class (This Report)	21. No. of Pages
Release Unlimited	UNCLASSIFIED	
	20. Security Class (This Page)	22. Price
	UNCLASSIFIED	

3D BEAM-COLUMN ELEMENT
(TYPE 2 - PARALLEL ELEMENT THEORY)
FOR THE ANSR-II PROGRAM

by

Ali Riahi
Graduate Student

Graham H. Powell
Professor of Civil Engineering

and

Digambar P. Mondkar
Assistant Research Engineer

Report to
National Science Foundation

Report No. UCB/EERC - 79/31
Earthquake Engineering Research Center
College of Engineering
University of California
Berkeley, California

ABSTRACT

This report describes a three dimensional inelastic beam-column element developed for the ANSR-II program. The report contains a description of the element characteristics, the theoretical formulation, and a computer program user's guide.

ACKNOWLEDGEMENTS

This work has been performed under the sponsorship of the National Science Foundation, Grant No. ENV 76-04262. The computing facilities were provided by the Computer Centers of the University of California, Berkeley and the Lawrence Berkeley Laboratory.

TABLE OF CONTENTS

1. INTRODUCTION

This report describes a three-dimensional beam-column element for the ANSR-II [1] program. The element has the following features:

(1) Arbitrary orientation in space.

(2) Plastic hinges can form only at the element ends.

(3) Plastic hinge formation governed by two bending moments, torsion and axial force.

(4) Trilinear action-deformation relationship for each of the four actions.

(5) Eliptical or parabolic yield surface.

(6) Different yield strengths at the two ends if desired. Different strengths for axial tension and compression.

(7) Rigid joint zones if desired.

(8) Initial forces in the element if desired.

(9) Rigid diaphragm slaving at any one or both ends of the element if desired.

(10) Shear deformations may be included or ignored.

(11) For dynamic analysis, damping proportional to initial elastic stiffness and/or current tangent stiffness.

(12) P-delta effect may be considered ("second order" analysis), but not true large displacements.

This report contains a description of the element and the element user's guide.

2. THREE DIMENSIONAL BEAM – COLUMN ELEMENT

2.1 GENERAL CHARACTERISTICS

Three dimensional beam-column elements may be arbitrarily oriented in the global XYZ plane. If the slaving feature is to be used, the Y axis must be vertical.

Each element must be assigned flexural stiffness and axial stiffness. Plastic hinges can form at the element ends. Interaction among the bending moments, torsional moment and axial forces at a hinge are taken into account in determining when hinges form. Displacements are assumed to be small, although the P-delta effect may be considered.

The orientation of the local element axes is as shown in Fig. 2.1. Node k, together with nodes i and j, defines the plane containing the local y axis.

Trilinear relationships can be specified for the moment-rotation relationship about the element y axis (M_y-θ_y), moment-rotation about the element z axis (M_y-θ_z), torque-twist (T-ϕ), and force extension (F-ε) for the element, as indicated in Fig. 2.2. Different yield strengths can be specified at the two ends if desired. Different strengths can also be specified for axial tension and axial compression.

Each element is automatically divided into three parallel elements, two of which are elastic-perfectly plastic and the third elastic. The stiffnesses and strengths of these parallel elements are calculated by the program such that the action-deformation relationships for the combined element have the specified trilinear forms. Each elastic-perfectly-plastic parallel element may develop a concentrated plastic hinge, with zero lengths, at one or both ends. The forces at each potential hinge interact according to one of two available yield functions to produce yield. The two available functions define elliptical and parabolic yield surfaces, as shown in Fig. 2.3. The origin of the yield surface may be shifted along the force axis, as shown, so that the surface can be made to approximate that for a reinforced concrete column.

Elements with varying strengths can be modelled by specifying different action-deformation relationships at the two element ends, but the element stiffness is assumed to be constant along the element length. Shear deformations may be included; however, interaction effects with shear are ignored. Eccentric end connections, initial forces, and rigid diaphragm slaving may be specified.

2.2 TANGENT STIFFNESS FOR AN ELASTO-PLASTIC PARALLEL COMPONENT

A tangent stiffness matrix can be derived which relates increments in the element end actions to increments in the element deformations for a single parallel component. That is,

$$\underline{dS} = \underset{\sim}{k}_t \, \underline{dv} \tag{2.1}$$

in which dS = vector of element action increments,

$\underline{dv}$ = vector of element deformation increments, and

$\underset{\sim}{k}_t$ = element tangent stiffness matrix.

The following basic assumptions are necessary for development of the theory:

(a) Element deformation increments can be decomposed into elastic and plastic components. That is,

$$\underline{dv} = \underline{dv}_e + \underline{dv}_p \tag{2.2}$$

in which $\underline{dv}_e$ = vector of elastic deformation increments, and

$\underline{dv}_p$ = vector of plastic deformation increments.

(b) Element action increments are related to the elastic deformation increments by the elastic action-deformation relationship. That is,

$$\underline{dS} = \underline{k}_e \, \underline{dv}_e \tag{2.3}$$

in which $\underline{k}_e$ = initial elastic stiffness matrix.

(c) The plastic increment of deformation is normal to the yield surface, directed outwards. For a hinge, at, say, element end i, this assumption can be expressed as:

$$\underline{dv}_{pi} = \underline{\phi}_{i,s} \cdot \lambda_i \tag{2.4}$$

in which $\phi_{i,s}$ = gradient vector of yield function at end i, each term being a partial derivative of the yield function with respect to the corresponding element action, and λ_i = a (positive) scalar which determines the magnitude of the plastic deformations.

With these three assumptions, the tangent stiffness matrix for an element with hinges at either or both ends is formed as follows.

For the hinges at ends i and j, from Eq. 2.4,

$$\underline{dv}_{pi} = \underline{\phi}_{i,s} \cdot \lambda_i \tag{2.5a}$$

and

$$\underline{dv}_{pj} = \underline{\phi}_{j,s} \cdot \lambda_j \tag{2.5b}$$

Eqs. 2.5a and 2.5b can be combined to give

$$\begin{Bmatrix} \underline{dv}_{pi} \\ \underline{dv}_{pj} \end{Bmatrix} = \begin{bmatrix} \underline{\Phi}_{i,s} & \underline{0} \\ 0 & \underline{\Phi}_{j,s} \end{bmatrix} \begin{Bmatrix} \lambda_i \\ \lambda_j \end{Bmatrix} \tag{2.6}$$

or

$$\underline{dv}_p = \underline{\Phi}_{,s} \, \underline{\lambda} \tag{2.7}$$

At each hinge, the value of the yield function must remain constant. That is,

$$d\phi_i = 0 \tag{2.8a}$$

and

$$d\phi_j = 0 \tag{2.8b}$$

or

$$\underline{\Phi}_{i,s}^{T} \cdot d\underline{S}_i = 0 \tag{2.9a}$$

and

$$\underline{\Phi}_{j,s}^{T} \cdot \underline{dS}_j = 0 \tag{2.9b}$$

Eqs. 2.9a and 2.9b can be combined to give

$$\begin{bmatrix} \underline{\Phi}_{i,s} & \underline{0} \\ 0 & \underline{\Phi}_{j,s} \end{bmatrix}^{T} \begin{Bmatrix} \underline{dS}_i \\ \underline{dS}_j \end{Bmatrix} = 0 \tag{2.10}$$

or

$$\underline{\phi}^T_{,s} \cdot \underline{dS} = \underline{0} \tag{2.11}$$

Substitution of Eq. 2.2 into Eq. 2.3 gives

$$\underline{dS} = \underline{k}_e(\underline{dv} - \underline{dv}_p) \tag{2.12}$$

and substitution of Eq. 2.7 into Eq. 2.12 gives

$$\underline{dS} = \underline{k}_e(\underline{dv} - \underline{\phi}_{,s}\, \underline{\lambda}) \tag{2.13}$$

Premultiplication of Eq. 2.13 by $\underline{\phi}^T_{,s}$ gives

$$\underline{\phi}^T_{,s}\, \underline{dS} = \underline{\phi}^T_{,s}\, \underline{k}_e(\underline{dv} - \underline{\phi}_{,s}\, \underline{\lambda}) \tag{2.14}$$

Hence, from Eq. 2.11

$$\underline{\phi}^T_{,s}\, \underline{k}_e(\underline{dv} - \underline{\phi}_{,s}\, \underline{\lambda}) = \underline{0} \tag{2.15}$$

or

$$(\underline{\phi}^T_{,s}\, \underline{k}_e\, \underline{\phi}_{,s})\underline{\lambda} = (\underline{\phi}^T_{,s}\, \underline{k}_e)\underline{dv} \tag{2.16}$$

Eq. 2.16 can be solved for $\underline{\lambda}$ to give

$$\underline{\lambda} = (\underline{\phi}^T_{,s}\, \underline{k}_e\, \underline{\phi}_{,s})^{-1}\, (\underline{\phi}^T_{,s}\, \underline{k}_e)\underline{dv} \tag{2.17}$$

It can be shown that for certain cases, in particular when an element is yielding at both ends under axial force alone or under torque alone, the determinant of $\underline{\phi}^T_{,s}\, \underline{k}_e\, \underline{\phi}_{,s}$ is zero. That is, the two simultaneous equations represented by Eq. 2.16 are linearly dependent. For such cases, it can be assumed that the plastic deformation magnitudes at ends i and j (i.e., λ_i and λ_j) are equal. This assumption avoids the singularity.

Substitution of Eq. 2.17 into Eq. 2.13 yields the elasto-plastic stiffness relationship

$$\underline{dS} = \left[\underline{k}_e - (\underline{k}_e \underline{\phi}_{,s}) (\underline{\phi}^T_{,s} \underline{k}_e \underline{\phi}_{,s})^{-1} (\underline{\phi}^T_{,s} \underline{k}_e)\right] \underline{dv} \qquad (2.18)$$

or

$$\underline{dS} = \underline{k}_t \, \underline{dv} \qquad (2.19)$$

which is the required tangent stiffness relationship.

From equilibrium of axial forces and torques, it follows that

$$dF_i = dF_j. \qquad (2.20a)$$

and

$$dT_i = dT_j \qquad (2.20b)$$

where F and T denote axial force and torque, respectively. Eqs. 2.20 must hold in all situations, whether an element yields at one or both ends and whether there are equal or different yield strengths at the two ends. This requirement suggests that six element degrees of freedom can be used, as shown in Fig. 2.5, rather than the eight shown in Fig. 2.4. A theory similar to that outlined above can be derived, with the 8-by-2 matrix $\underline{\phi}_{,s}$ compacted into a 6-by-2 matrix such that Eq. 2.11 still holds. Using this modified matrix, the increments of plastic axial and torsional deformation, as computed by Eq. 2.7, become the combined plastic deformations at both hinges.

Compaction from eight degrees of freedom to six has the advantage of reducing the computational effort. The formulation with six degrees of freedom is used in the computer program.

The preceding derivation can be applied to the case with only one plastic hinge as well as the case with two hinges. For an element with one hinge, the column of the matrix $\underline{\phi}_{,s}$ corresponding to the elastic end becomes zero and is deleted. The vector $\underline{\lambda}$ then becomes a scalar.

2.3 TOLERANCE FOR STIFFNESS REFORMULATION

Each time a new hinge forms or an existing hinge unloads, the element stiffness changes. Moreover, because the yield surface is curved, the stiffness of a yielding element will generally change continuously. This change in stiffness results from differences in the directions of the tangents to the yield surface as the actions at the hinge change, as shown in Fig. 2.6 for successive states. If the angle α is small, the change in stiffness is small and can be neglected, to avoid recalculating the stiffness. In the computer program, an option is provided for the user to set a tolerance for the angle α. If a nonzero tolerance is specified, the element stiffness is reformed only when the change in state is such that the angle between the current state and that at which the stiffness was last reformed exceeds the tolerance. For computational reasons, the program computes α by adding the absolute values of changes in α over succeeding steps. This is conservative, but provides a reasonable measure of the true angle.

Tangent stiffnesses for each of the two inelastic parallel elements are computed according to the preceding theory. These stiffnesses are then added together, and further added to the stiffness of the elastic parallel element.

2.4 P-DELTA EFFECT

Even for small displacements, changes in the shape of a structure can have a significant effect (the P-delta effect) on the equilibrium of the structure. This effect can be accounted for by adding a geometric stiffness to the element elastic or elasto-plastic stiffness, and by accounting for change of shape in the calculation of the resisting force for the element.

The geometric stiffness assumed for the element is that for a truss bar in three dimensions, which depends on the axial force only. The geometric stiffness is changed each time the elasto-plastic stiffness changes, using the current axial force, but is otherwise assumed to remain constant.

The effect of including the geometric stiffness is to account approximately (linearized or "second order" approximation) for large displacement effects. A corresponding correction is included in the state determination calculations, by modifying the resisting forces exerted by the element on the nodes at its ends. The modification adds shear forces to the nodes, based on the element axial force and its chord rotation (Δ/h).

2.5 STATE DETERMINATION FOR AN ELASTO-PLASTIC PARALLEL COMPONENT

Increments of the element end actions are computed from Eq. 2.3. For an element with elastic ends, $\underline{dv}_e$ is equal to $\underline{dv}$. For an element with one or two plastic hinges, $\underline{dv}_e$ is obtained from Eq. 2.2. The plastic deformation, $\underline{dv}_p$ is obtained from Eq. 2.4 after first computing $\underline{\lambda}$ by Eq. 2.17. A negative value of λ for any end indicates that unloading has occurred at that end. If a plastic hinge unloads the matrix, $\underline{\phi}_{,s}$ is recalculated without the hinge before applying the above equations.

During any load step, the element end actions may move outside the yield surface. This is not admissible and must be corrected. As an example, consider Fig. 2.7 showing paths which the actions at ends i and j might take during a single step. At the beginning of the step, the actions are at points A, end i being elastic and end j plastic. Assuming linear behavior within the step, the final actions would be at points B. However, these actions are outside the yield surfaces at both ends, which is not correct.

It is assumed, first, that the actions reach points B along straight lines from A to B (that is, the deformations increase proportionately from A to B). The action points C, along lines AB, are then obtained by computing the portion of the deformation increment which just brings end i to yield. The actions at end j, as shown by point C, will be slightly outside the yield surface because the true behavior at end j is not linear. These actions are scaled to give point D on the yield surface, along the line joining C to the centroid of the yield surface. At this stage, the actions at both ends are on the yield surface, at points D. For the remainder of the deformation increment, hinges are present at both ends. The increments in element actions are computed, giving points E. Again, the actions are not exactly on the yield surface. A further correction is therefore made by scaling the actions to give points F.

The actions for each of the parallel elements are calculated in this way and are then added together to give the total element actions. Plastic deformations, consisting of plastic hinge rotations, twists, and extensions at each end, are also calculated. Because there are two elasto-plastic elements in parallel, two different sets of plastic deformations are present. The deformations printed by the program are those for the parallel element which yields first. The deformations for the other element are not printed.

2.6 END ECCENTRICITY

Plastic hinges in frames and coupled frame-shear wall structures will form near the faces of the joints rather than at the theoretical joint centerlines. This effect can be approximated by specifying rigid, infinitely strong connecting links between the nodes and the element ends, as shown in Fig. 2.8. The displacement transformation relating the increments of node displacements, dr_n, to increments of displacements at the element ends is easily established, and can be written as

$$\underline{dv} = \underline{a}_e \, \underline{dr}_n \tag{2.21}$$

The element tangent stiffness is then transformed as follows:

$$\underline{K} = \underline{a}_e^T \, \underline{K}_t \, \underline{a}_e + \underline{K}_G \tag{2.22}$$

where $\underline{K}_G$ is included only if geometric stiffness is to be considered. Note that the geometric stiffness is based on a truss bar connecting the theoretical joint centerlines directly.

2.7 RIGID FLOOR SLAVING

A frequently made assumption in the analysis of tall buildings is that each floor diaphragm is rigid in its own plane. To model this assumption, a "master" node at the center of mass of each floor may be specified, as shown in Fig. 2.9. Each master node has three degrees of freedom as shown, which are the displacements of the diaphragm as a rigid body. If any beam-column member is connected to a diaphragm, its stiffness must be formulated partly in terms of these "master" displacements and partly in terms of displacements which are not affected by the rigid diaphragm assumption.

The displacement transformation relating the diaphragm displacements, $\underline{dr}_d$, to the displacements at a slaved node is as follows:

$$\begin{Bmatrix} dr_{n1} \\ dr_{n3} \\ dr_{n5} \end{Bmatrix} = \begin{bmatrix} 1 & 0 & d_z \\ 0 & 1 & -d_x \\ 0 & 0 & 1 \end{bmatrix} \begin{Bmatrix} dr_x \\ dr_z \\ dr_\theta \end{Bmatrix} \tag{2.23}$$

or

$$\underline{dr}_{ns} = \underline{a}_d \, \underline{dr}_d \qquad (2.24)$$

The slaved displacements at element nodes i and j can be expressed in terms of the displacements at the "master" node (or nodes). The corresponding coefficients of $\underline{K}$ (eq. 2.22) are transformed to account for the slaving. The resulting element stiffness matrix is assembled in terms of the three master degrees of freedom plus the three local degrees of freedom dr_{n2}, dr_{n4}, and dr_{n6} at each node, which are not affected by slaving.

2.8 INITIAL FORCES

For structures in which static analyses are carried out separately (i.e., outside the ANSR program), initial member forces may be specified. These forces are not converted to loads on the nodes of the structure, but simply used to initialize the element end actions. For this reason, initial forces need not constitute a set of actions in equilibrium. The only effects they have on the behavior of the system are (a) to influence the onset of plasticity and (b) to affect the geometric stiffnesses.

Initial forces are defined as patterns. Each element can then be identified with an initial force pattern. The sign convention for positive initial forces is shown in Fig. 2.10.

2.9 RESULTS OUTPUT

The following response results are printed at the specified output intervals in static and dynamic analyses, for those beam-column elements for which response results are requested.

(1) Element number.

(2) Node numbers at ends i and j.

(3) Yield codes for ends i and j. This code is as follows for each end:

00: both elasto-plastic parallel elements are elastic.

10: only one of the elasto-plastic parallel elements is plastic.

11: both elasto-plastic parallel elements are plastic.

(4) Moments about the element y and z axes, at each end, and torque and axial force. Positive directions of the actions are shown in Fig. 2.11.

(5) Plastic hinge rotations about the element y and z axes, plastic hinge twist, and plastic hinge axial extension for each end of the element. Positive directions of the plastic deformations are shown in Fig. 2.11.

Envelope values of results (i.e., maximum positive and negative values of results and the corresponding times at which they occur) can also be printed if requested.

3. USER'S GUIDE

3D BEAM COLUMN ELEMENT (TYPE 2)

3.1 CONTROL INFORMATION - Two cards

3.1(a) First Card

COLUMNS	NOTE	NAME	DATA
5(I)		NGR	Element group indicator. Punch 2.
6 - 10(I)	(1)	NELS	Number of elements in group.
11 - 15(I)		MFST	Element number of first element in group. Default = 1.
16 - 25(F)		DKO	Initial stiffness damping factor, β_o .
26 - 35(F)		DKT	Current tangent stiffness damping factor, β_T .
41 - 80(A)		GRHED	Optional group heading.

3.1(b) Second Card

COLUMNS	NOTE	NAME	DATA
1 - 5(I)		NMBT	Number of different strength types (max. 20). Default = 1.
6 - 10(I)		NECC	Number of different end eccentricity types (max. 15). Default = zero.
11 - 15(I)		NPAT	Number of different initial force patterns (max. 30). Default = zero.

3.2 STRENGTH TYPES

NMBT sets of cards, four cards per set.

3.2(a) Bending Properties about Local y-axis.

COLUMNS	NOTE	NAME	DATA
1 - 5(I)			Strength type number, in sequence beginning with 1.
6 - 15(F)			Flexural stiffness (effective elastic EI value, K1) about y axis.
16 - 25(F)			Flexural stiffness (K2) about y-axis.

3.2(a) Bending Properties about Local y-axis (continued)

COLUMNS	NOTE	NAME	DATA
36 - 45(F)	(2)		Yield moment (YS1) about y-axis.
46 - 55(F)			Yield moment (YS2) about y-axis.
56 - 65(F)			Elastic shear stiffness (GA_s) for bending about y-axis. May be zero.

3.2(b) Bending Properties about Local z-axis

COLUMNS	NOTE	NAME	DATA
1 - 5			Blank.
6 - 65(F)			z-Axis bending stiffnesses, yield moments and shear stiffness, in the same sequence as in card 3.2(a).

3.2(c) Torsional Properties

COLUMNS	NOTE	NAME	DATA
1 - 5			Blank.
6 - 55(F)			Torsional stiffnesses (effective GJ) and yield moments, in same sequence as in card 3.2(a).

3.2(d) Axial Properties

COLUMNS	NOTE	NAME	DATA
1 - 5			Blank.
6 - 55(F)			Axial stiffnesses (effective EA) and yield forces, in the same sequence as in card 3.2(a).
56 - 65(F)	(3)		Yield force (YS3). Input as a positive value. Default = YS1.

3.3 END ECCENTRICTIY TYPES

NECC cards.

COLUMNS	NOTE	NAME	DATA
1 - 5(I)	(4)		End eccentricity type number, in sequence beginning with 1.
6 - 15(F)			X_i = X eccentricity at end i.
16 - 25(F)			X_j = X eccentricity at end j.
26 - 35(F)			Y_i = Y eccentricity at end i.
36 - 45(F)			Y_j = Y eccentricity at end j.
46 - 55(F)			Z_i = Z eccentricity at end i.
56 - 65(F)			Z_j = Z eccentricity at end j.

3.4 INITIAL ELEMENT FORCE PATTERNS

NPAT cards.

COLUMNS	NOTE	NAME	DATA
1 - 5(I)	(5)		Pattern number, in sequence beginning with 1.
6 - 15(F)			Initial moment M_{yy} at end i.
16 - 25(F)			Initial moment M_{zz} at end i.
26 - 35(F)			Initial moment M_{yy} at end j.
36 - 45(F)			Initial moment M_{zz} at end j.
46 - 55(F)			Initial axial force, F.
56 - 65(F)			Initial torque M_{xx} .

3.5 ELEMENT DATA GENERATION

As many cards as needed to generate all elements in group.

COLUMNS	NOTE	NAME	DATA
1 - 5(I)	(6)		Element number, or number of first element in a sequentially numbered series of elements to be generated by this card.
6 - 10(I)		NODI	Node number I.

3.5 ELEMENT DATA GENERATION (Continued)

COLUMNS	NOTE	NAME	DATA
11 - 15(I)		NODJ	Node number J.
16 - 20(I)		INC	Node number increment for element generation. Default = 1.
21 - 25(I)	(7)		Number of a third node, K, lying in the xy plane, for definition of the local y axis orientation. Default = automatic orientation of y-axis.
26 - 30(I)			Number of node (diaphragm node) to which end I is slaved (NSI). Default = no slaving.
31 - 35(I)			Number of node to which end J is slaved (NSJ). Default = no slaving.
36 - 40(I)			Strength type number at element end i. No default.
41 - 45(I)			Strength type number at element end j. No default.
46 - 50(I)			End eccentricity type number. Default = no end eccentricity.
51 - 55(I)			Initial Force pattern number. Default = no initial forces.
60(I)			Interaction surface type. (a) 1 = elliptical surface. (b) 2 = parabolic surface.
65(I)			Small displacements code. (a) Blank or zero = small displacements. (b) 1 = large displacements ("second order" analysis).
70(I)			Response output code. (a) Blank or zero = no response printout. (b) 1 = response output required.
71 - 80(F)	(8)		Stiffness reformulation angle tolerance, α (radians). Default = zero.

3.6 USER'S GUIDE NOTES

NOTE (1) The elements in the group are numbered sequentially, starting with MFST (i.e., MFST, MFST + 1, ... , MFST + NELS - 1).

NOTE (2) The action-deformation relationships for y-axis bending, z-axis bending, torsion and axial force need not necessarily be geometrically similar (e.g., the ratio YS2/Ys1 for y-axis bending may be different from that for z-axis bending). However, it is generally advisable to make the relationships nearly similar.

NOTE (3) The value of YS3 allows the origin of the yield surface to be shifted along the P-axis. The strengths in pure tension and compression are then different, and the yield surface approximates that for a reinforced concrete column. Note that the yield force, YS4, in compression (Fig. 2.2) is not specified, because it is assumed that YS4 - YS3 = YS2 - YS1.

NOTE (4) All eccentricities are measured from the node to the element end (Fig. 2.8), positive in the positive coordinate directions.

NOTE (5) See Fig. 2.10 for the positive directions of initial element actions. Refer to Section 2.8 for a description of the effects of initial element actions.

NOTE (6) Cards must be input in order of increasing element number. Cards for the first and the last elements must be included (that is, data for these two elements cannot be generated).

Cards may be provided for all elements, in which case each card specifies the data for one element, and the generation option is not used. Alternatively, cards for a series of elements may be omitted, in which case data for the missing elements is generated as follows:

(a) All missing elements are assigned the sane node "K" (NODK), slave nodes (NSI and NSJ), strength types, end eccentricity type, initial force pattern type, interaction surface type, codes for small displacements and response output, and stiffness reformulation angle tolerance, as for the element preceding the missing series of elements.

(b) The node numbers I and J for each missing element are obtained by adding the increment (INC) to the node numbers of the preceding element. That is,

$$NODI(N) = NODI(N - 1) + INC$$

$$NODJ(N) = NODJ(N - 1) + INC$$

Node increment (INC) is the value specified with the element preceding the missing series of elements.

NOTE (7) The element y-axis is oriented in a plane passing through nodes I and J and a third node K (Fig. 2.1). Note that the node K must not be collinear with nodes I and J. If a third node is not specified, the element y-axis is assumed to be in a plane which is parallel to the global Y-axis and passes through nodes I and J (typically, the vertical plane containing the element), with a positive projection on the Y-axis. If the element is parallel to the global Y-axis, then this default procedure does not work, and the element y-axis is assumed to be parallel to the global X-axis.

NOTE (8) Refer to Section 2.3 for a description of the stiffness reformulation tolerance.

REFERENCE

1. Mondkar, D.P. and Powell, G.H., "ANSR-II, Analysis of Nonlinear Structural Response, User's Manual", Report No. UCB/EERC-79/17, Earthquake Engineering Research Center, University of California, Berkeley (July 1979).

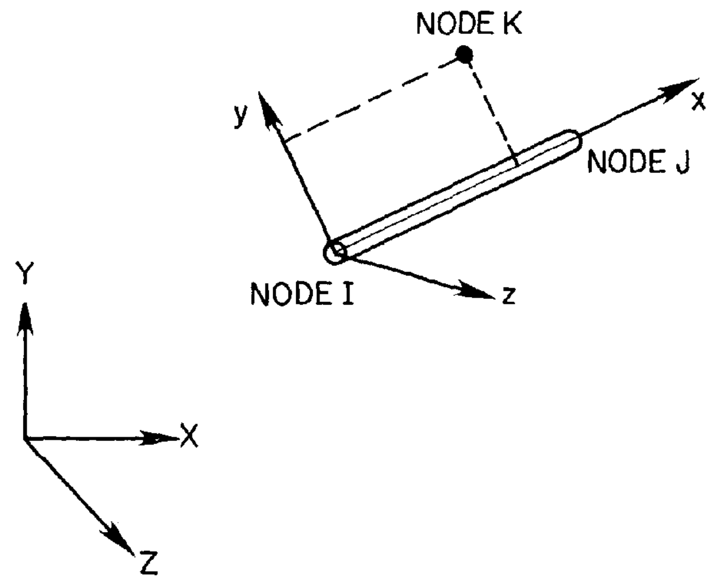

FIG. 2.1 ELEMENT COORDINATE AXIS

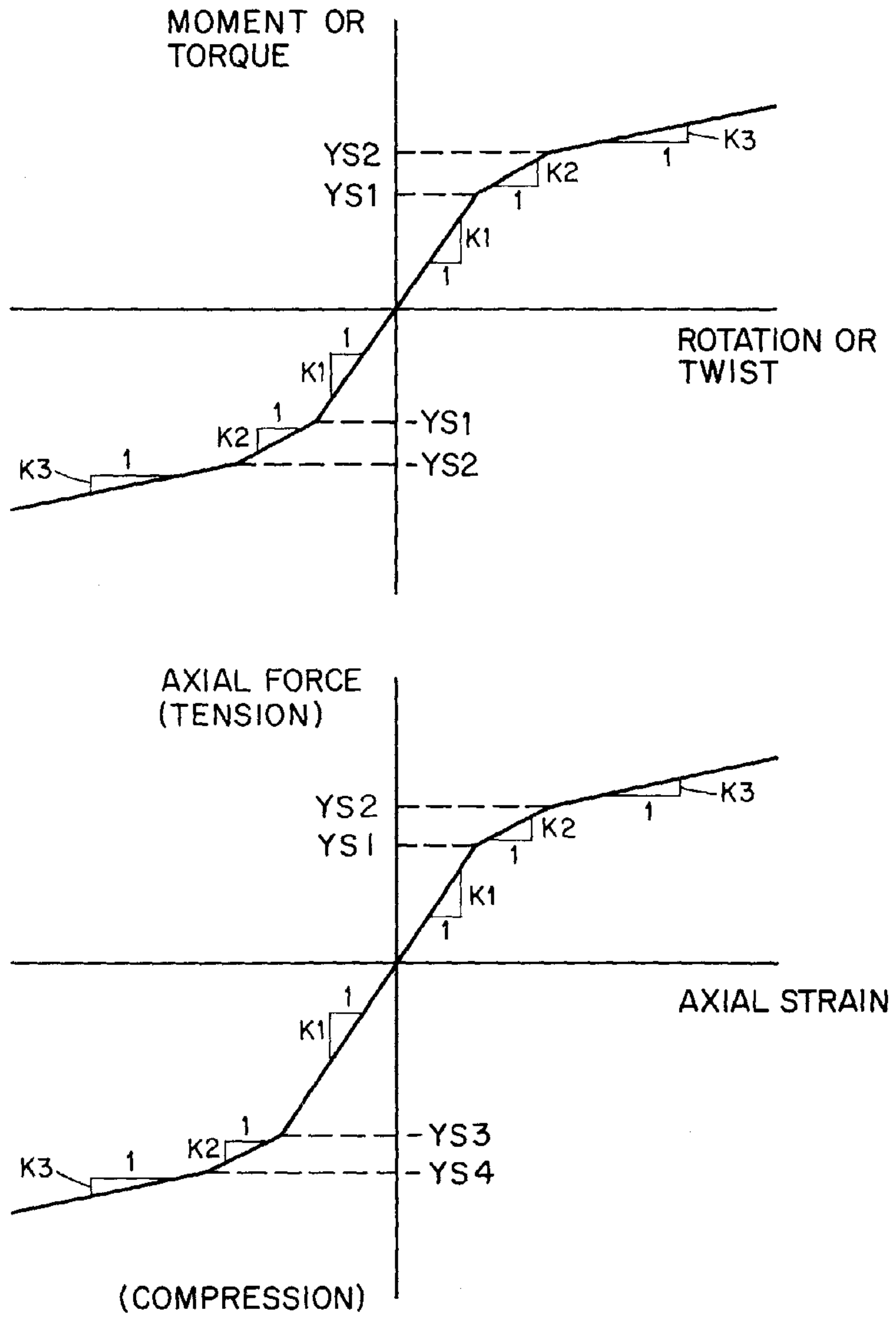

FIG. 2.2 ACTION-DEFORMATION RELATIONSHIPS

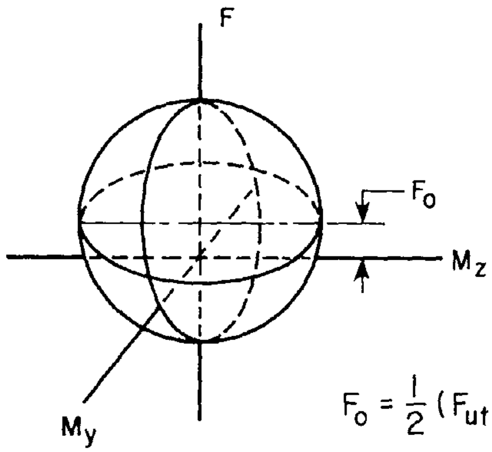

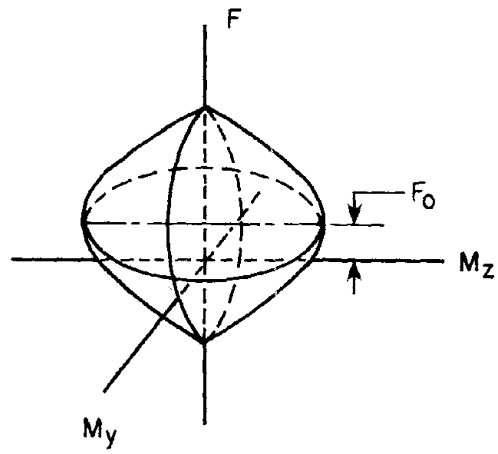

$$F_o = \frac{1}{2}(F_{ut} - F_{uc})$$

$$F_u = \frac{1}{2}(F_{ut} + F_{uc})$$

$$\phi = \left(\frac{M_y}{M_{yu}}\right)^2 + \left(\frac{M_y}{M_{zu}}\right)^2 + \left(\frac{T}{T_u}\right)^2 + \left(\frac{F-F_o}{F_u}\right)^2 = 1$$

INTERACTION SURFACE TYPE 1

$$\phi = \left[\left(\frac{M_y}{M_{yu}}\right)^2 + \left(\frac{M_z}{M_{zu}}\right)^2 + \left(\frac{T}{T_u}\right)^2\right]^{1/2} + \left(\frac{F-F_o}{F_u}\right)^2 = 1$$

INTERACTION SURFACE TYPE 2

M_y, M_z, T and F denote bending moments about the element y and z axes, torque and axial force respectively. Subscript u denotes ultimate. F_{ut} and F_{uc} are axial ultimate strengths in tension and compression. Note that the interaction surfaces above are for a particular value of torque, T.

FIG. 2.3 INTERACTION SURFACES FOR ELASTO-PLASTIC COMPONENT

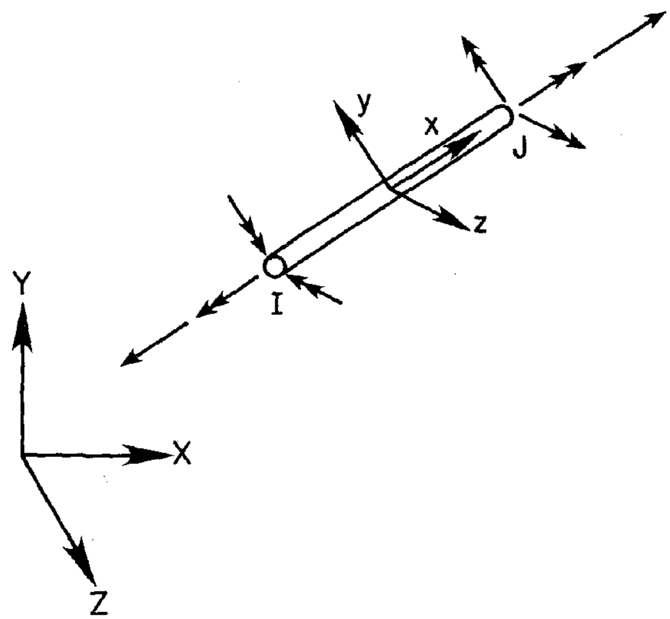

FIG. 2.4 ELEMENT NODAL FORCES AND DEFORMATIONS

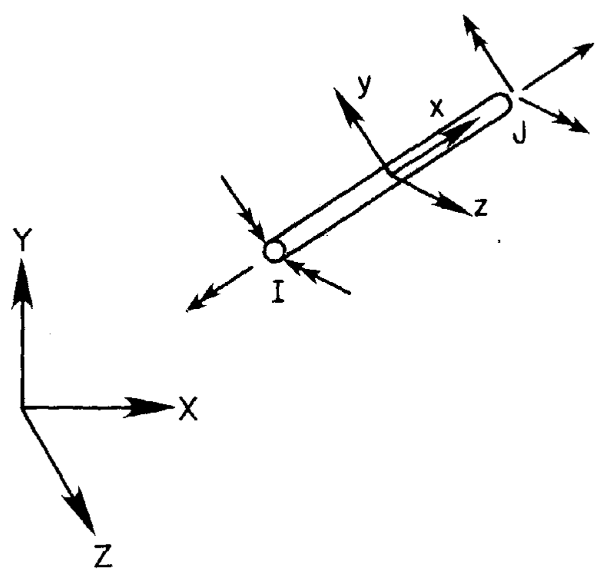

FIG. 2.5 COMPACTED ELEMENT NODAL FORCES AND DEFORMATIONS

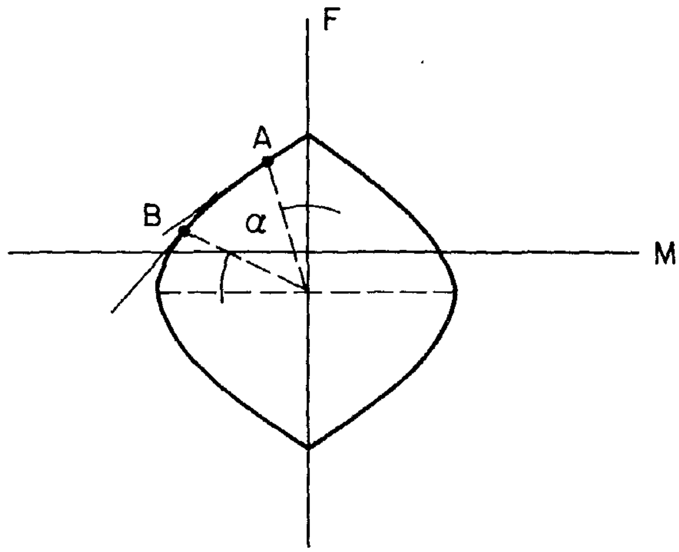

FIG. 2.6 STIFFNESS REFORMULATION ANGLE

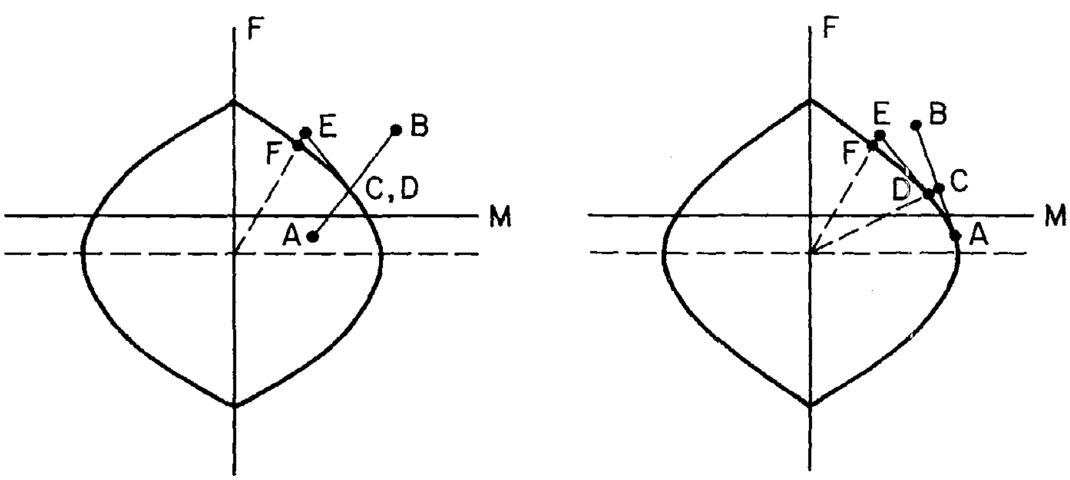

YIELD SURFACE AT END I   YIELD SURFACE AT END J

FIG. 2.7 STATE DETERMINATION EXAMPLE

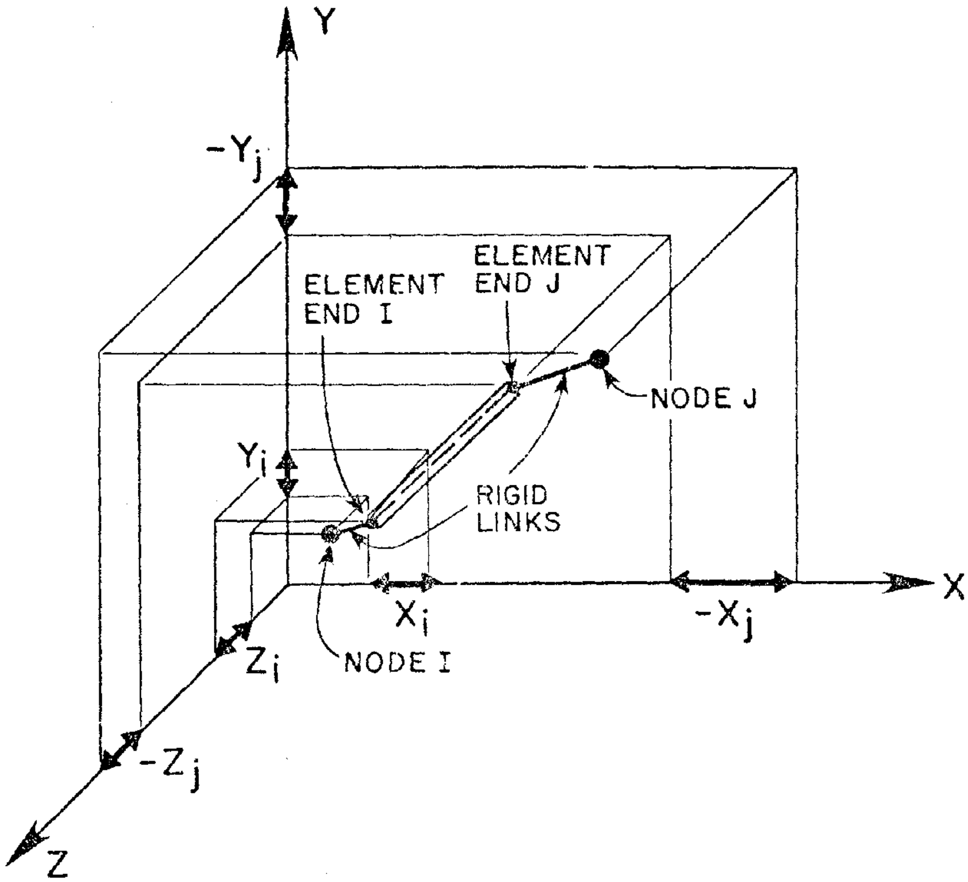

FIG. 2.8 END ECCENTRICITIES

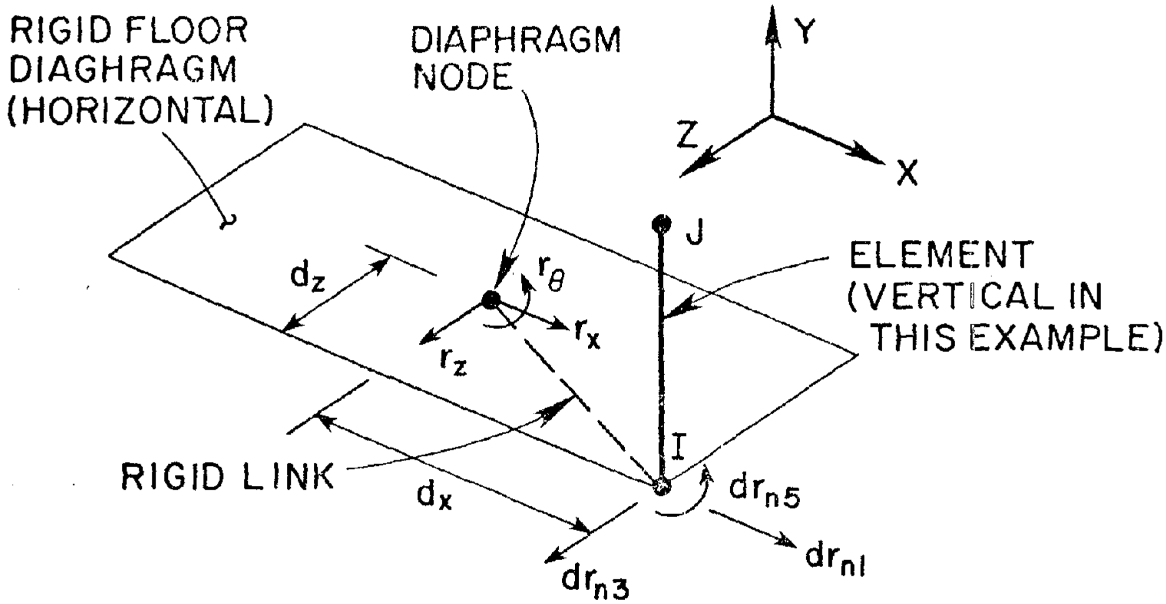

FIG. 2.9 RIGID FLOOR DIAPHRAGM MODELLING

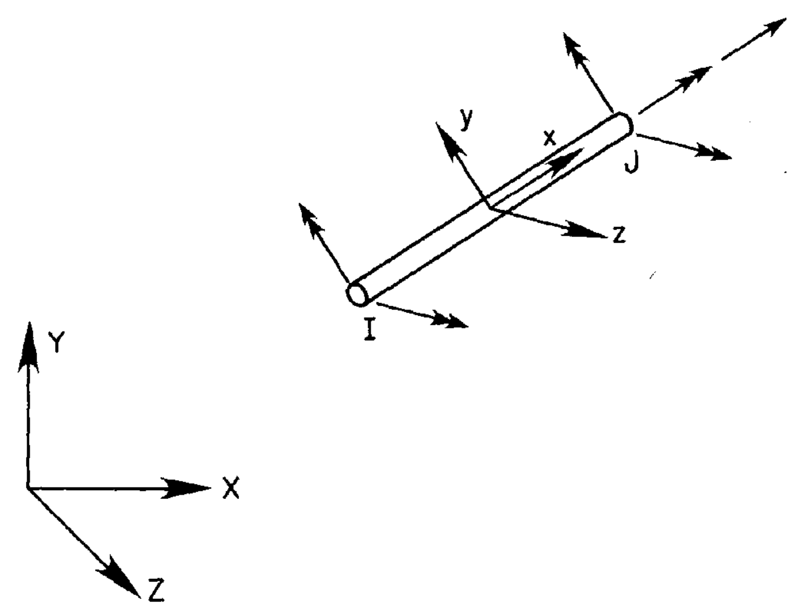

FIG. 2.10 POSITIVE DIRECTION OF INITIAL ELEMENT ACTIONS

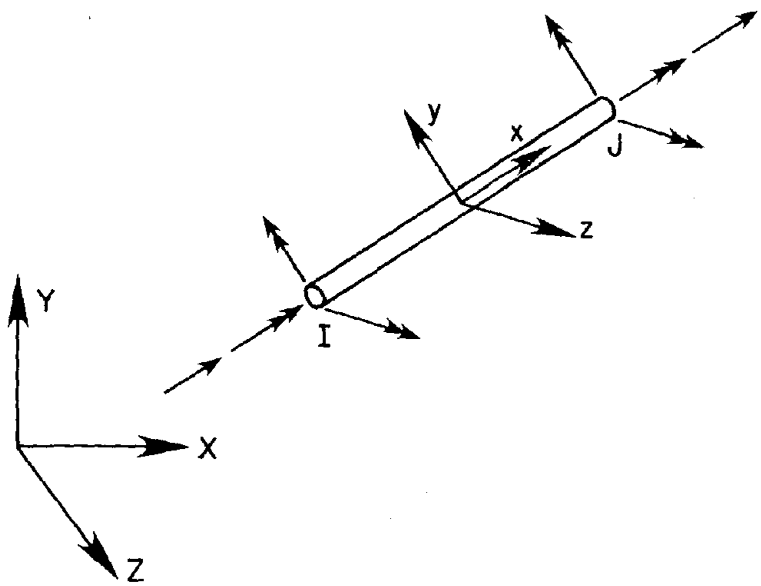

FIG. 2.11 POSITIVE DIRECTION OF NODAL FORCES AND DEFORMATION FOR OUTPUT RESULTS